CYBERNETICS AND PHYSICS, VOL. 6, NO. 1, 2016 , 5–12

EXPERIMENTAL STUDY OF MULTIRESONANCE MECHATRONIC VIBRATIONAL LABORATORY SET-UP

Boris Andrievsky
Control of Complex Systems Lab
Institute of Problems of
Mechanical Engineering of RAS
ITMO University
Saint Petersburg, Russia
boris.andrievsky@gmail.com

Vladimir I. Boikov
Computer Science and Control Systems Dept
ITMO University
Saint Petersburg, Russia
viboikov@mail.ru

Abstract

In the paper, the properties of the novel mechatronic set-up – the Vibration Stand are studied. The set-up consists of a spring-suspended platform with electrically driven unbalanced rotors, a personal computer for control of the stand and processing the data of experiments, set of sensors, computer interface facilities and an amplification-transformation unit. The experimental results are presented and compared with the simulation ones to demonstrate the motor parameter identification and PI-control of the unbalanced rotors angular velocity. The angular velocity control system in the frequency domain is experimentally studied and the Sommerfeld effect is demonstrated. The set-up may be widely used for development of new technologies in the manufacturing industry as well for physical researches and the education.

Key words

Nonlinear, mechatronic set-up, vibration, stand, technology.

1 Introduction

Mechatronic devices needs simultaneous coordinated functioning of mechanical, electronic, software and control subsystems. They afford to researchers appropriate experimental facilities allowing to implement modern project-based technologies. A number of the research laboratory set-ups for relatively simple and traditional units are described in the literature: for motors (Pogromsky and Van Den Berg, 2014), active vibration suspension systems (Arias-Montiel *et al.*, 2014), pendulum-like oscillators (Andrievsky and Fradkov, 1999; Fradkov *et al.*, 2005; Fradkov *et al.*, 2014; Oud *et al.*, 2006), etc. However there are only a few set-ups with multiple DOF systems allowing to study and demonstrate complex nonlinear behavior (Fradkov *et al.*, 2012; Mayr *et al.*, 2015; Panovko *et al.*, 2015). The testbed of (Panovko *et al.*, 2015) includes a rigid rectangular platform, horizontally installed on 14 identical springs and two unbalanced vibro-actuators. The wider range of research work, including both open-loop and closed-loop control of vibrations, may be fulfilled with the help of the Vibration Stand *SV-2*[1], designed in the IPME RAS jointly with the Mekhanobr Engineering JSC (Andrievskii *et al.*, 2016; Andrievsky *et al.*, 2016; Boikov *et al.*, 2016; Fradkov *et al.*, 2016). This set-up makes it possible to study and demonstrate the various phenomena which arise in mechanical units, such as the phenomenon of self-synchronization, the Sommerfeld effect, start up of the unbalanced rotors rotation, the passage through the resonance area, the closed-loop control of the synchronization, vibration isolation and chatter suppression (Tomchin and Fradkov, 2007; Tomchina and Kudryavtseva, 2005). In (Fradkov *et al.*, 2016), the SV-2 is used to experimentally demonstrate that the suggested by the authors feedback control law allows rotors to overcome gravity and to start rotation by means of a low level control action. An important application is the development of new technologies for the manufacturing, based on the implementation of computer control. Quite a number of applications are related to education in mechanical and electrical engineering, automatic control, computer science, signal processing, and so on.

Using the theoretical and experimental results, obtained with the help of the SV-2 allows to improve the efficiency of existing vibration machines and to develop a new generation of high-production vibration devices for various branches of the industry, especially for such as mining, metallurgy and chemical industries, as well as production of new materials with the desired properties.

[1] Initially named in (Andrievskii *et al.*, 2016) as "*the Multiresonance Mechatronic Laboratory Set-up* (MMLS)".

The SV-2 includes a vibration stand, electrical engines, sensors, and a personal computer (PC). All the devices constitute an integrated system, where the electrical and mechanical processes are inextricably linked each other, which gives a basis to call the set-up a *mechatronic* one.The mechanical part of the SV-2 is an electrically driven vibration device. Stand SV-2 can operate in two modes: the *self-synchronization* mode and the *controlled synchronization* one. Using the vibroactuators' self-synchronization phenomenon makes possible to obtain various types of vibrations of the stand frame by changing the rotors turning direction. However, the self-synchronization mode for some cases is not quite stable: random deviations of the motor parameters and settings, as well as fluctuations of technological load can cause large changes of the phase difference of the rotor turning from the values which ensure the desired mode of oscillation. In other cases, the required phasing of rotor rotation is unstable. In these situations the problem of motor control arises, where the measurement of the rotor angles is also needed, and an influence of the relative phase shift of rotation, i.e. operation in the controlled synchronization mode should be taken into account.

This paper is devoted to the experimental study of the SV-2. This study allowed us to reveal a number of interesting properties of the set-up demonstrating it complex nonlinear behavior. The experiments on parameter identification of the motors, interacting with vibrating frame; rotational frequency PI-controller design and testing; experimental study of the angular velocity control system in the frequency domain and demonstration of the Sommerfeld effect have been carried out and are described in the present work below.

The rest of the paper is organized as follows. Brief description of the set-up, including its general structure, mechanical, electrical parts and software support is given in Sec. 2. Section 3 presents the results of motor parameters identification and rotational frequency PI-controller design and testing. Results of experimental evaluation in the frequency domain for the angular velocity control system are given in Sec. 4. The Sommerfeld effect is demonstrated in Sec. 5. Concluding remarks and the discussion of the future work are given in Sec. 6.

The SV-2 consists of the *vibration stand*, a pair of the *induction motors* with *unbalanced rotors*, the *electronic converter amplifier*, the *sensor assembly* with the special *controller* for signal processing, and the *personal computer*, supplied with the devices for *interface* with the hardware.

2 Mechatronic Set-up Description

2.1 Mechanical Part of the Set-up: The Vibration Stand

The general view of the SV-2 is demonstrated in Fig. 1. The key part of the set-up is a vibration stand, including a pair of the unbalanced (centrifugal) actuators, driven by computer-controlled three-phase AC induction motors. Unbalance of the rotor is provided by the eccentrically located weight. Upon rotation of the unbalanced rotors around their axes, the centrifugal forces arise, which are summarized in a certain way, forming the desired vibration modes with various forms of the trajectories for different points of the base. In more details the stand is described in (Andrievskii *et al.*, 2016; Andrievsky *et al.*, 2016; Boikov *et al.*, 2016).

Figure 1. General view of the SV-2.

2.2 Electrical and Electronic Devices of the Set-up

The stand is equipped with five optical sensors measuring the table and the extra weight positions, velocity sensors with a resolution of 1000 pulses/revolution for two independently rotating rotors, as well as with the sensors of electric motor current. Set of the sensors can serve as a source of signals for studying and demonstrating the measuring systems, the signal processing, and the real-time control. Signals from the sensors are used not only for generating motor control signals, but also for keeping the set-up vibrations within safe limits. For stand table and the extra weight positions measurement, the assemblies including eight linear and angular displacement sensors are installed. Each platform bears three angular and three linear optical encoders. Measured data from all the 12 sensors are transmitted to the PC. The stand security system also includes protection of power electrical short-circuit, the thermal protection, and the protection of people against electric shock.

Schematics of electronic pert of the SV-2 is presented in Fig. 2. The SV-2 includes the PC, supplied with the interface card PCI826 and *ICP DAS PISO Encoder600* — 1, *Schneider Electric* frequency converter *Altivar ATV12H018M2* — 2; two asynchronous motor *5A50MA2* — 3; unbalanced rotors — 4; the *AUTONICS* encoders *E30S4-1000-6L* — 5; the mobile platforms – primary (m_1) and the secondary ones (m_2); the optical sensors measuring platforms displacement — 6. The control circuit diagram is shown in Fig 3.

2.3 Software Support

Real-time data processing and control are carried out by means of Simulink Desktop Real-Time™ of

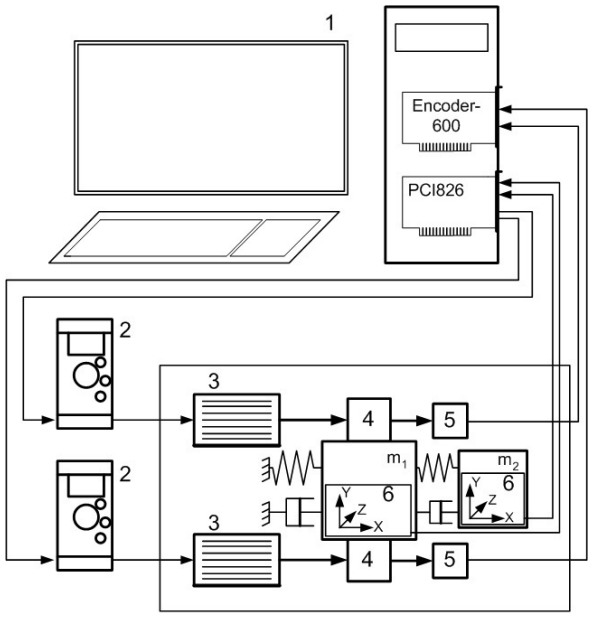

Figure 2. SV-2 schematics: 1 – PC with the interface card and encoder; 2 – frequency converter; 3 – asynchronous motor; 4 – unbalanced rotor; 5 – encoder; m_1, m_2 – primary and secondary mobile platforms; 6 – optical sensor.

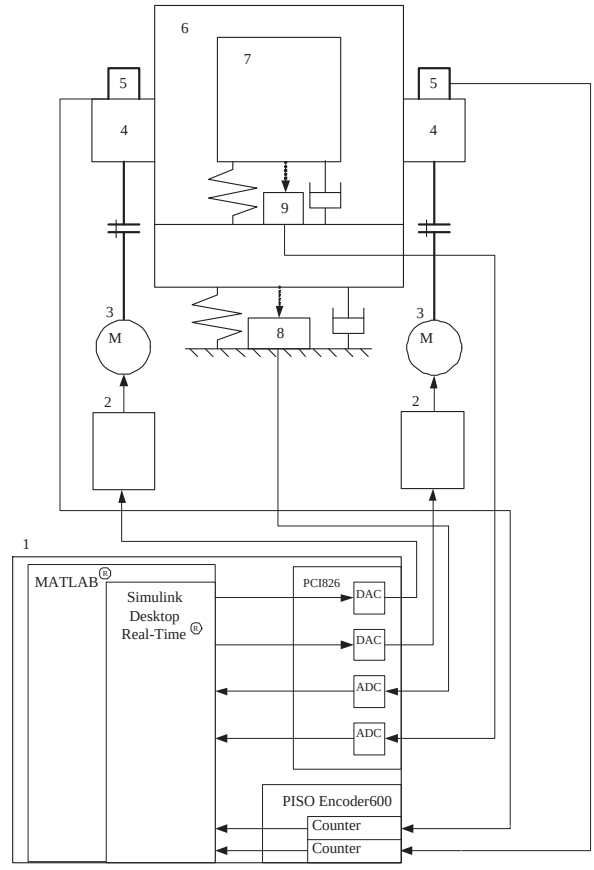

Figure 3. The control circuit diagram: 1 – PC; 2 – frequency converter; 3 – asynchronous motors; 4 – unbalanced rotors; 5 – encoder; 6 – primary vibration platform; 7 – secondary vibration platform; 8, 9 – optical sensors.

MATLAB© R2015b software. Control signal computation can be performed with a sampling rate up to 1000 Hz. In parallel, time histories of the chosen variables may be displayed on the PC monitor. To provide a researcher with a fast and convenient way for performing the experiments with the SV-2, the programming interface based on the Simulink Toolbox™ was created. A typical example of the Simulink block-diagram for experiments is shown in Fig. 4. The following blocks are used in the Simulink diagram for experiments with the PI-controlled rotational frequency:

– *Constant1*, *Pulse Generator* constitute the source of the reference signal for both motors in the form of a biased 'square wave' ('meander'). The reference rotational frequency is given in radians per second. In this example the bias is set to 80 rad/s;
– *Kp1*, *Kp2* are the proportional gains of PI-controllers for the 'left' and 'right' (conventionally) motors. In the presented example they both are set to 1036 s/rad;
– *KI1*, *KI2* are the integral gains of PI-controllers. In our example they both are set to 396 1/rad;
– *Integrator*, *Integrator Limited1* are the blocks for computing the integral parts of the PI control actions. Integrating is fulfilled by means of the Euler method with the constant step time h, equal to the sampling time T_s of the overall control system (for our experiments $h = 10$ ms is taken). The integrator states are bounded by the interval $[0, 65535]$ for preventing the wind-up effect;
– *Sum* units form the control actions. In the model, the angular velocity controls are measureless integer numbers from the interval $[0, 65535]$, as follows from the design features of the interface card PCI826, which is used in the SV-2;
– *PCI1* is the Simulink model graphical representation of the interface card PCI826. Two input signals are the control actions, formed by the PI-controllers in the form of 16-bits integer numbers from the interval $[0, 65535]$. Three vector output sihnals represent 18 signals of the set-up analogue sensors, represented as integers from the interval $[0, 65535]$. Analogue-to-digital conversion takes $4\ \mu$s;
– *PISO1* is the graphical representation of the driver for encoders E30S4-1000-6L. Driver output signals are the rotation angles in 32-bits integer representation. Single revolution of the rotor gives an encoder output value equal to 4000. Therefore, the encoder scaling factor K_e is defined as $K_\mathrm{e} = 2\pi/4000 \approx 0.00157$ rad;
– *Data Type Conversion*, . . . ,*Data Type Conversion6* are the service blocks which are used for transforming the data format of the encoder outputs to

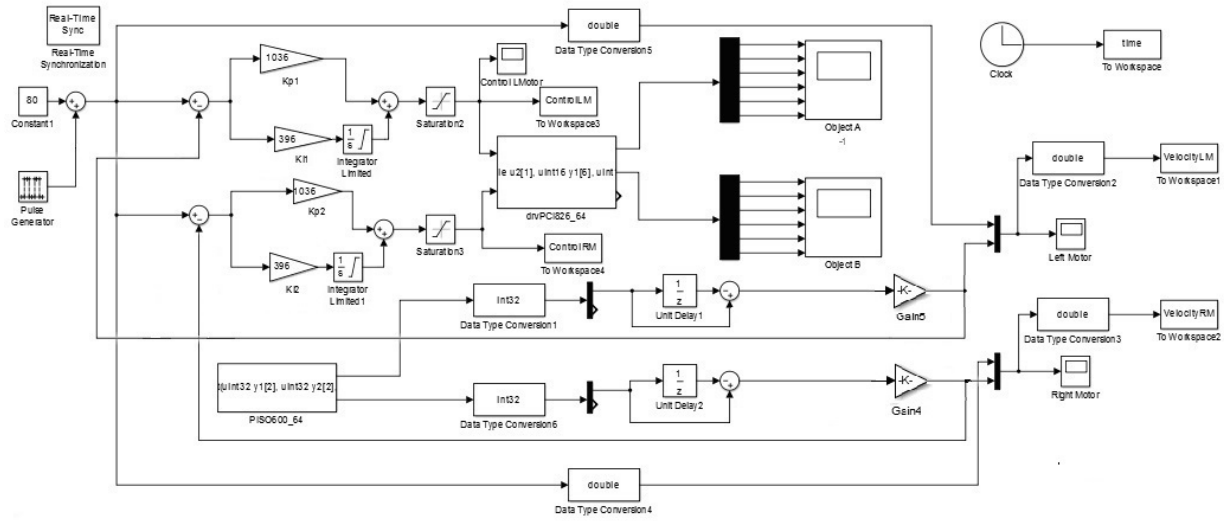

Figure 4. Simulink block-diagram

Simulink numerical format;

- *Unit Delay1*, *Unit Delay2* are one-step time-delay blocks which are used for numerical differentiation of the rotation angles for computing the rotor angular velocities;
- *Gain5*, *Gain4* are the scaling gains transforming the angular velocity signals to rad/s. Since the sampling time $T_s = 0.01$ s is taken, then the gains are as $K_e/T_s = 0.157$ rad/s;
- *Real-Time Synchronization* block is used for setting the common sampling time T_s in the system. $T_s = 0.01$ s is set.
- *To Workspace*, *To Workspace1*, *To Workspace2* blocks serve for recording the experimental data to the MATLAB workspace for further processing. Usually the data are saved by a user in the dedicated *.mat* file.

3 Computer Control of the Vibration Stand

3.1 Tuning the PI-controller to the Magnitude Optimum

The input of the frequency converter is fed by the dimensionless digital control signal u from the range of $[0, 65000]$, the measured output is angular velocity ω of the unbalanced rotor. At the present stage of the work, the PI-controllers in the angular velocity control loops are used. To find the controller gains an approximate model of the drive (including the frequency converter, induction motor, and the unbalanced rotor) is taken in the form of the second order aperiodic link with one large and one small time constants, which leads to the following plant transfer function from u to ω:

$$W_p(s) = \frac{K_d}{(Ts+1)(\tau s+1)}, \qquad (1)$$

where K_d denotes the plant static gain, T and τ are "large" (dominant) and "small" time constant, respectively.

The linearized model (1) parameters of the asynchronous motor significantly depend on the operating conditions. In the present study the operating angular velocity as 50 rad/s has been taken. With the help of MATLAB routine *fminsearch*, implementing the direct search Nelder-Mead simplex algorithm, the following parameter values, minimizing the mean-square error between the time histories, obtained experimentally and via the simulations, have been found: $K_d = 0.0032$ rad/s, $T = 2.62$ s, $\tau = 0.40$ s (for the 'right' motor), and $K_d = 0.0032$ rad/s, $T = 3.0$ s, $\tau = 0.16$ s (for the 'left' motor).

Let us use the proportional-integral (PI) control law for rotor angular velocity control. The PI-controller transfer function from tracking error to the control action has a form

$$W_c(s) = K_p + \frac{K_i}{s} = K_i \frac{T_c s + 1}{s}, \qquad (2)$$

where K_p, K_i are the proportional and integral controller gains (respectively), and equivalent time constant T_c is introduced as $T_c = \dfrac{K_p}{K_i}$, $s \in \mathbb{C}$ denotes the Laplace transform variable.

Let us use the magnitude optimum (MO) design method (Åström and Hägglund, 1995; Vrančić *et al.*, 2001) for choice the PI-controller parameters. Following this method, T_c is taken equal to T, which leads to compensation of dominant time constant T. Consequently, $K_p = TK_i$. Therefore, after equal pole and zero cancellation, the closed-loop system transfer function $\Phi(s)$ from the reference (desired) rotation fre-

quency ω^* to the actual one, ω, may be represented as

$$\Phi(s) = \frac{K_i K_d}{\tau s^2 + s + K_i K_d}. \tag{3}$$

For the considered system, the MO condition reads $(K_i K_d)^{-1} = 2\tau$, which leads to the following expression for integral gain K_i:

$$K_i = \frac{1}{2\tau K_d}. \tag{4}$$

Taking into account the above-stated parameter values for the left motor, one finally obtains the PI-controller gains as $K_i = 396$ 1/rad, $K_p = 1036$ s/rad.

Let us mention that for the considered case the MO design method leads to the transient time (with respect to 2% zone around the steady-state value) as $t_{\text{fin}} = 8.4\tau = 3.3$ s and overshoot σ as 4.3 %.

3.2 Simulation and Experimental Results

The simulations and the experiments have been carried out for reference rotation frequency ω^* as 60 rad/s and 120 rad/s. For the experiments, measurements and control computation have been performed with a rate 100 Hz. The results for the left motor are depicted in Figs. 5, 6.

Time histories of $\omega_l(t)$, $u_l(t)$, obtained via the simulation ($\omega_{l\text{sim}}$, $u_{l\text{sim}}$) and the experiment ($\omega_{l\text{exp}}$, $u_{l\text{exp}}$) for reference value $\omega^* = 60$ rad/s are plotted in Fig 5. Figure 6 corresponds the case of $\omega^* = 120$ rad/s.

The results obtained show that the MO design method gives the satisfactory results for the real-world system, and the simulation results are close to the experimental ones. Note that in the presented experiments no Sommerfeld effect (Blekhman, 2000*b*) occurs. The stand gives an opportunity to experimentally investigate the control systems under the conditions where this effect is significant. Such experiments are planned for the future.

It should be noticed that as $\omega^* > 60$ rad/s, the control input is saturated at the beginning of the process, which increases the transient time and the overshoot. Such a phenomenon, known as a *windup effect* may be suppressed by means of the appropriate anti-windup compensation technique, cf. (Tarbouriech *et al.*, 2011).

4 Experimental Evaluation of the Angular Velocity Control System in the Frequency Domain

The performance analysis of linear control systems is essentially based on frequency domain characteristic such as *sensitivity function* $A_e(\Omega)$ which is defined for harmonic reference signal $r(t) = A \sin \Omega t$ of magnitude A and frequency Ω as a relative magnitude of the steady-state error e to the reference signal magnitude A. In the literature (Pogromsky and Van Den

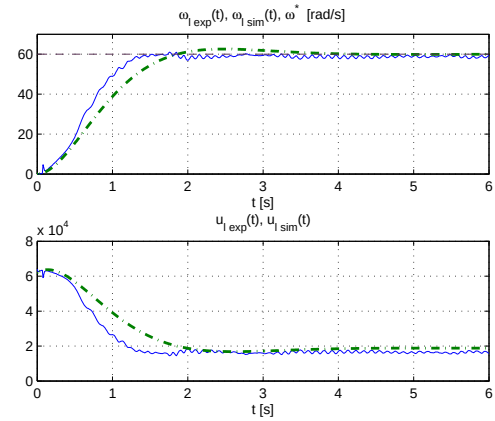

Figure 5. Time histories of $\omega_l(t)$ (upper plot), $u_l(t)$ (lower plot) as $\omega^* = 60$ rad/s. $\omega_{l\text{exp}}$ – solid line, $\omega_{l\text{sim}}$ – dash-dot line, ω^* – dashed line; $u_{l\text{exp}}$ – solid line, $u_{l\text{sim}}$ – dash-dot line.

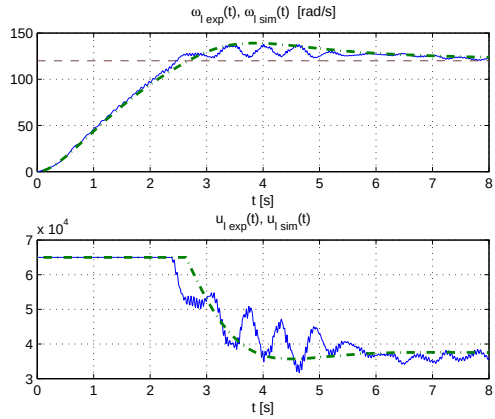

Figure 6. Time histories of $\omega_l(t)$ (upper plot), $u_l(t)$ (lower plot) as $\omega^* = 120$ rad/s. $\omega_{l\text{exp}}$ – solid line, $\omega_{l\text{sim}}$ – dash-dot line, ω^* – dashed line; $u_{l\text{exp}}$ – solid line, $u_{l\text{sim}}$ – dash-dot line.

Berg, 2014), for nonlinear Lur'e systems, possessing convergence property the generalized version of this function is also defined as

$$S_e(\Omega) = \|e\|_2 / \|r\|_2, \tag{5}$$

where $\|z\|_2 = \left(\frac{\omega}{2\pi} \int_0^{2\pi/\omega} z(\tau)^2 \, d\tau\right)^{1/2}$. For the linear case, function $S_e(\Omega)$ coincides with customary amplification frequency characteristic $A_e(\Omega)$. For nonlinear systems, function $S(\Omega)$ depend not only on the excitation frequency Ω, but also on the amplitude A.

To evaluate sensitivity functions $A_e(\Omega)$, $S_e(\Omega)$ of the angular velocity control system experimentally, the biased harmonic reference signal

$$\omega^*(t) = 60\left(1 - e^{-2t}\right) - 20 \sin \Omega t \tag{6}$$

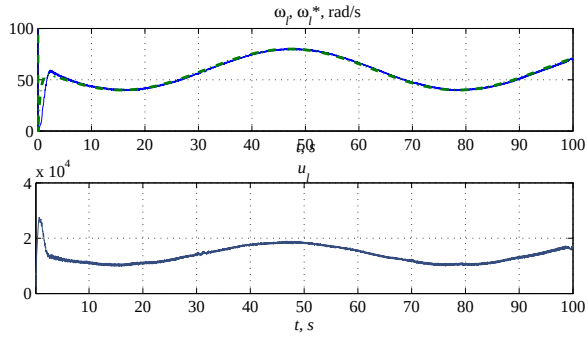

Figure 7. Time histories of $\omega_l(t)$ – solid line, $\omega^*(t)$ – dash-dot line (upper plot), $u_l(t)$ (lower plot). Harmonic reference signal (6), $\Omega = 0.1$ rad/s.

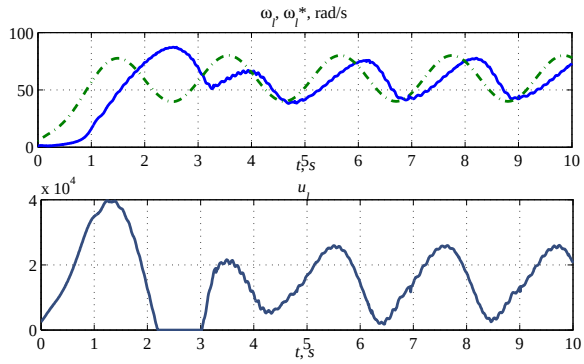

Figure 8. Time histories of $\omega_l(t)$ – solid line, $\omega_l^*(t)$ – dash-dot line (upper plot), $u_l(t)$ (lower plot). Harmonic reference signal (6), $\Omega = 3.0$ rad/s.

with various Ω has been applied to the closed-loop system. The bias of the reference ω^* (in 60 rad/s for our case) is needed since only one rotational direction may be reproduced by the AC motors of the SV-2 and available rotation frequency ω is bounded, see Sec. 5. An exponential multiplier for the bias of 60 rad/s has been used for avoiding intensive transients at the beginning of the process. The sample time histories of the left motor angular velocity $\omega_l(t)$ for $\Omega = 0.1, 3.0$ rad/s are plotted in Figs. 7, 8. The plots show that the transient time of the closed-loop system with PI-controller (2) and gains $K_i = 396$ 1/rad, $K_p = 1036$ s/rad does not exceed 5 s (cf. Figs. 5, 6). The experimentally obtained sensitivity functions for $\Omega \in [0.1, 6.0]$rad/s are depicted in Fig. 9. As follows from the results, the range of tracking the harmonic reference signal (6) is bounded by $\Omega = 0.25$ rad/s, where $S_e(\Omega) = 0.1$.

5 Demonstration of the Sommerfeld Effect

A typical problem for control of vibration units is passing through resonance at start-up mode of vibroactuators, in the case of the operating modes belonging to a post-resonance zone. Such a problem arises in the case when the power of a motor is not sufficient for passage through resonance zone due to the

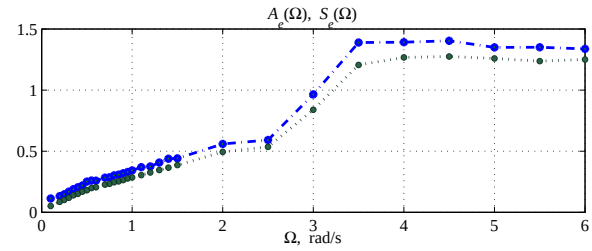

Figure 9. Experimental results in frequency domain. $A_e(\Omega)$ – dash-dot line, '$*$', $S_e(\Omega)$ – dotted line, 'o'.

so-called *Sommerfeld effect*, cf. (Sommerfeld, 1902; Blekhman, 1988; Blekhman *et al.*, 1995; Blekhman, 2000*a*; Blekhman, 2016; Kovriguine, 2012). This effect consists of influence of the lateral motion of the unbalanced shaft support on its rotation, mainly in the vicinity of a resonance. At resonance vibrational motion provides just an 'energy sink', or, as Sommerfeld put it 'the plant owner spends expensive coal not to rotate his shaft, but rather to shake the foundation' (Sommerfeld, 1902; Dimentberg *et al.*, 1997).

For checking a possibility of the Sommerfeld effect on the SV-2, the steady-state values of the rotational frequency ω as a function of control action u have been experimentally found. To this end, the various constant values of the control have been applied to the motors in the open-loop, and after finishing the transients, ω was recorded. The results for the left motor ($u = u_l$, $\omega = \omega_l$) are plotted in Fig. 10. The plot shows that in the open loop and the steady-state mode, the rotation frequency does not exceeds 132 rad/s, despite the control action is increased up to its maximal value. Simultaneously, resonant oscillations of the carrying frame with a significant magnitude arise, which indicates appearance of the Sommerfeld effect. The other feature of an open-loop control is presence of the threshold: rotational velocity is close to zero if the control action is less 13000. If the threshold is overcome, then the steady-state frequency rapidly increases. This phenomenon is explained, mainly, the pendulum properties of the unbalanced rotor – small rotation torque can not compensate the gravity torque, acting to the unbalance, cf. (Dimentberg *et al.*, 1997; Åström and Furuta, 2000; Fradkov *et al.*, 2002; Fradkov *et al.*, 2005; Fradkov *et al.*, 2016).

Operating properties of the vibration stand may be essentially improved by applying the feedback control. An example is demonstrated by the plot in Fig. 11, where tracking the linearly increasing reference signal ω_l^* by means of the closed-loop PI-controlled system is demonstrated. In the open loop, the rotational frequencies up to 60 rad/s could not been achieved with an appropriate precision due to the mentioned pendulum swinging effect, as shown in Fig. 10. In the contrary, PI-controller ensures precise steady-state velocity control in the range of $[40, 120]$ rad/s, see Fig. 11.

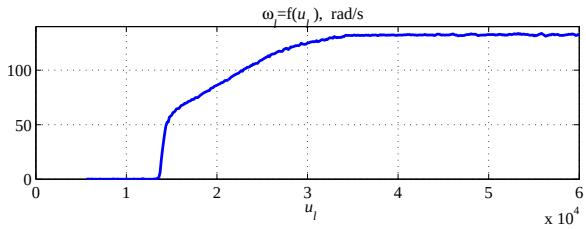

Figure 10. Steady-state values of the rotational frequency ω_l as a function of control action u_l in the open-loop system. Presence of the threshold and the Sommerfeld effect.

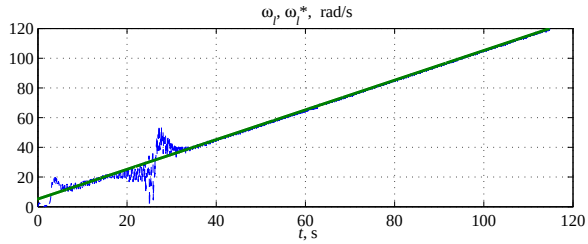

Figure 11. Tracking the linearly increasing reference signal in the closed-loop. PI-controller (2), $K_i = 396$ 1/rad, $K_p = 1036$ s/rad. $\omega_l(t)$ – dashed line, $\omega_l^*(t)$ – solid line.

Rotational frequencies less than 40 rad/s can not be controlled due to a very strong resonant interaction between the unbalanced rotors and the oscillating frame on the low frequencies. The other possible application of the closed-loop control may be in overcoming the Sommerfeld effect. In the future it is planned to examine the existing theoretical results in this field (Tomchin and Fradkov, 2005; Tomchin and Fradkov, 2007; Fradkov *et al.*, 2011; Fradkov *et al.*, 2016) on the SV-2.

6 Conclusions

A research mechatronic set-up – the SV-2, created in the IPME RAS, makes it possible to study and demonstrate the various phenomena which arise in mechanical units, such as the phenomenon of self-synchronization, the Sommerfeld effect, start up of the unbalanced rotors rotation, the passage through the resonance area,the closed-loop control of the synchronization, etc. In the paper we have demonstrated a number of phenomena that can be applied to development of new vibration technologies, vibration isolation and chatter suppression (Tomchin and Fradkov, 2007; Tomchina and Kudryavtseva, 2005). The field of the potential applications may be significantly extended by attaching the supplementary devices to the carrier body.

An important application is the development of new technologies for the manufacturing, based on the implementation of computer control. Quite a number of applications are related to education in mechanical and electrical engineering, automatic control, computer science, signal processing, and so on.

Using the theoretical and experimental results, obtained with the help of the SV-2 allows to improve the efficiency of existing vibration machines and to develop a new generation of high-production vibration devices for various branches of the industry, especially for such as mining, metallurgy and chemical industries, as well as production of new materials with the desired properties. The stand may be also widely used for studying the physical properties of bulk solids subjected by vibrations, as well as in the studying the physical phenomena in vibrational mechanical systems.

Acknowledgment

The work was partially supported by the Government of Russian Federation, Grant 074-U01. The multiresonance mechatronic laboratory set-up Vibration Stand (SV-2) has been created in the IPME RAS under the financial support of the Russian Science Foundation (project 14-29- 00142).

References

Andrievskii, B. R., I. I. Blekhman, L. I. Blekhman, V. I. Boikov, V. B. Vasil'kov and A. L. Fradkov (2016) Education and research mechatronic complex for studying vibration devices and processes. *J. Mach. Manuf. Reliab.*, **45**(4), pp. 369–374. (translated from original Russian text published in Problemy Mashinostroeniya i Nadezhnosti Mashin, 2016, No. 4, pp. 91–97).

Andrievsky, B. R. and A. L. Fradkov (1999) Feedback resonance in single and coupled 1-DOF oscillators. *Int. J. Bifurcations and Chaos*, **10**, pp. 2047–2058.

Andrievsky, B., V. I. Boikov, A. L. Fradkov and R. E. Seifullaev (2016) Mechatronic laboratory setup for study of controlled nonlinear vibrations. In: *Prepr. 6th IFAC International Workshop on Periodic Control Systems (PSYCO 2016)* (H. Nijmeijer and A. Pogromsky, Eds.). IFAC. TUe, Eindhoven, The Netherlands.

Arias-Montiel, M., G. Silva-Navarro and A. Antonio-García (2014) Active vibration control in a rotor system by an active suspension with linear actuators. *J. Applied Research and Technology*, **12**, pp. 898–907.

Åström, K.J. and K. Furuta (2000) Swinging up a pendulum by energy control. *Automatica*, **36**(2), pp. 287–295.

Blekhman, I. I. (1988) *Synchronization in Science and Technology*. ASME Press. New York.

Blekhman, I. I. (2000*a*) *Vibrational Mechanics*. World Scientific. Singapore. (Translated form original Russian text published in 1994).

Blekhman, I. I. (2000*b*) *Vibrational Mechanics: Nonlinear Dynamic Effects, General Approach, Applications*. World Scientific.

Blekhman, I. I. (2016) *Synchronization in Nature and Technology: Theory and Applications*. World Scientific. Singapore. (Translated from Russian ed., Nauka, Moscow, 1977).

Blekhman, I. I., P. S. Landa and M. G. Rosenblum (1995) Synchronization and chaotization in interacting dynamical systems. *Applied Mechanics Reviews*, **48**(11), pp. 733–752.

Boikov, V. I., B. Andrievsky and V. V. Shiegin (2016) Experimental study of unbalanced rotors synchronization of the mechatronic vibration setup. *Cybernetics and Physics*, **5**(1), pp. 5–11.

Dimentberg, M. F., L. McGovern, R. L. Norton, J. Chapdelaine and R. Harrison (1997) Dynamics of an unbalanced shaft interacting with a limited power supply. *Nonlinear Dynamics*, **13**, pp. 171–187.

Fradkov, A. L., B. Andrievsky and K. B. Boykov (2005) Control of the coupled double pendulums system. *Mechatronics*, **15**, pp. 1289–1303.

Fradkov, A. L., B. Andrievsky and K. B. Boykov (2012) Multipendulum mechatronic setup: Design and experiments. *Mechatronics*, **22**(1), pp. 76–82.

Fradkov, A. L., B. Andrievsky and M. S. Ananyevskiy (2014) State estimation and synchronization of pendula systems over digital communication channels. *Eur. Phys. J. Special Topics*, **223**, pp. 773–793.

Fradkov, A. L., B. R. Andrievsky and K. B. Boykov (2002) Numerical and experimental excitability analysis of multi-pendulum mechatronics system. In: *Proc. 15th IFAC World Congress*. Barcelona, Spain.

Fradkov, A.L., D. Gorlatov, O. Tomchina and D. Tomchin (2016) Control of oscillations in vibration machines: Start up and passage through resonance. *Chaos*, **26**(11), pp. 116310.

Fradkov, A.L, O.P. Tomchina and D.A. Tomchin (2011) Controlled passage through resonance in mechanical systems. *J. Sound and Vibration*, **330**(6), pp. 1065–1073.

Kovriguine, D. A. (2012) Synchronization and Sommerfeld effect as typical resonant patterns. *Arch. Appl. Mech.*, **82**, pp. 591–604.

Mayr, J., F. Spanlang and H. Gattringer (2015) Mechatronic design of a self-balancing three-dimensional inertia wheel pendulum. *Mechatronics*, **30**, pp. 1–10.

Oud, W. T., H. Nijmeijer and A. Yu. Pogromsky (2006) A study of Huijgens' synchronization: Experimental results. In: *Group Coordination and Cooperative Control; Lecture Notes in Control and Information Sciences* (K. Pettersen, J. Gravdahl and H. Nijmeijer, Eds.), **336**, pp. 191–203. Springer. Berlin.

Panovko, G. Ya., A. E. Shokhin and S. A. Eremeikin (2015) Experimental analysis of the oscillations of a mechanical system with self-synchronized inertial vibration exciters. *J. Mach. Manuf. Reliab.*, **44**(6), pp. 492–496. (translated from original Russian text published in *Problemy Mashinostroeniya i Nadezhnosti Mashin*, 2015, No. 6, pp. 11–15.).

Pogromsky, A. and R. Van Den Berg (2014) Frequency domain performance analysis of Lur'e systems. *IEEE Trans. Contr. Syst. Technol.*, **22**(5), pp. 1949–1955.

Åström, K. J. and T. Hägglund (1995) *PID controllers: Theory, design, and tuning*. Instrument Society of America Research Triangle Park (2nd ed.).

Sommerfeld, A. (1902) Beitrage zum dynamischen ausbau der festigkeislehre. *Z. Ver. Deut. Ing.*, **46**, pp. 391–394. (in German).

Tarbouriech, S., G. Garcia, J.M. Gomes da Silva Jr. and I. Queinnec (2011) *Stability and Stabilization of Linear Systems with Saturating Actuators*. Springer-Verlag. London.

Tomchin, D. A. and A. L. Fradkov (2005) Controlling passage of a rotor through the resonance band by the velocity-gradient method. *J. Machinery Manufacture and Reliability*, **5**, pp. 55–60.

Tomchin, D. A. and A. L. Fradkov (2007) Control of passage through a resonance area during the start of a two-rotor vibration machine. *J. Machinery Manufacture and Reliability*, **36**(4), pp. 380–385.

Tomchina, O. P. and I. M. Kudryavtseva (2005) Controlled synchronization of unbalanced rotors with flexible shafts in time-varying vibrational units. In: *Proc. IEEE-IUTAM Conf. on Physics and Control (PhysCon 2005)*. Saint Petersburg. pp. 790–794.

Vrančić, D., S Strmčnik and D. Juričić (2001) A magnitude optimum multiple integration tuning method for filtered PID controller. *Automatica*, **37**, pp. 1473–1479.